



Original

Moderate hyperglycemia suppresses melanoma metastasis to liver

Celine Swee May KHOO¹⁾, Tomohiro HATAKENAKA¹⁾, Nahoko MATSUKI¹⁾, Seiya MINAGAWA²⁾, Kyoka ASAMI²⁾, Takuya HENMI¹⁾, Akane MORIMOTO¹⁾ and Mikako SAITO^{1,3)}

¹⁾Department of Biotechnology and Life Science, Tokyo University of Agriculture and Technology, 2-24-16 Naka-cho, Koganei, Tokyo 184-8588, Japan

²⁾Department of Industrial Technology and Innovation, Tokyo University of Agriculture and Technology, 2-24-16 Naka-cho, Koganei, Tokyo 184-8588, Japan

³⁾Bioresource Laboratories, Tokyo University of Agriculture and Technology, 2-24-16 Naka-cho, Koganei, Tokyo 184-8588, Japan

Abstract: The metastasis of various cancers is promoted by hyperglycemia. In contrast, melanoma and colorectal cancer seemed to be exceptional. We confirmed that the metastasis of melanoma B16-F10 could be suppressed by hyperglycemia. It was attractive from the prognostic point of view of the prevention of metastasis, though the problem of the risk of diabetes remained. Then, the effect of moderate hyperglycemic condition was investigated using a pre-diabetic model mouse (GKKO mouse). The metastasis of B16-F10 cells to liver was focused and the number and volume of metastatic colonies in liver were analyzed. The medians of the number of metastatic colonies in GKKO mice were 0.57-fold ($P=0.06$) compared to control mice. Analysis of macrophage markers revealed upregulation of CD86, a tumor-suppressive M1-type marker, and downregulation of CD206, a tumor-promotive M2-type marker. A tendency of upregulation of Cxcl10, a pro-inflammatory cytokine was also observed. Regarding cellular activities of B16-F10, migration activity and invasion activity were reduced by moderate hyperglycemia. In conclusion, metastasis of B16-F10 cells to liver could be suppressed by moderate hyperglycemia without the risk of diabetes. This information should contribute to dietary planning during prognosis.

Key words: CD86, melanoma, metastasis suppression, moderate hyperglycemia, pre-diabetes model mouse

Introduction

Cancer is one of the global leading causes of death, and even with advanced treatment such as surgery and chemotherapy, metastasis still holds a threat to the prognosis of cancer patients. Melanoma is known to be prone to metastasis even in the early stages and to often recur and have a severe prognosis [1]. In addition, the incidence in Japan is increasing rapidly at the age of 60 and over. Therefore, reducing the risk of melanoma metastasis is an important issue in an aging society. Serious adverse effects might be caused by underlying diseases such as lifestyle-related diseases. Here, we focused on

diabetes as a lifestyle-related disease [2].

According to the Japan Diabetes Society (JDS) and the Japanese Cancer Association (JCA) [3], diabetes was reported to increase the risk of various cancers by about 0.84–2.5 fold. Hyperglycemia, the main symptom of diabetes is associated with the increase of reactive oxygen species and inflammatory markers [4], oxidative stress [5], and the increase of vascular permeability [6], which in all are reported to promote metastasis of pancreatic cancer [7, 8], lung adenocarcinoma [9], colorectal cancer [10], breast cancer [11], and colon cancer [12].

On the other hand, in the cases of melanoma and colorectal cancer, the suppression of growth or metasta-

(Received 2 June 2022 / Accepted 20 October 2022 / Published online in J-STAGE 27 October 2022)

Corresponding author: M. Saito. email: mikako@cc.tuat.ac.jp

Supplementary Table: refer to J-STAGE: <https://www.jstage.jst.go.jp/browse/expanim>



This is an open-access article distributed under the terms of the Creative Commons Attribution Non-Commercial No Derivatives (by-nc-nd) License <<http://creativecommons.org/licenses/by-nc-nd/4.0/>>.

sis was formerly reported [13, 14]. The growth of melanoma B16 in mice was retarded by hyperglycemia that was made by the administration of high concentrations of glucose or glucagon [13]. Similarly, the metastasis of colorectal cancer (CT 38, CT 26) in mice was suppressed by high-fat diet-induced hyperglycemia [14]. In contrast, the metastasis of colorectal cancer (CT 26) was promoted by streptozotocin (STZ)-induced hyperglycemia [10]. The different outcomes observed in colorectal cancer might be due to the difference in the ways of making hyperglycemic conditions.

A possibility of metastasis suppression effect observed in melanoma and colorectal cancer was thought to be attractive from the prognostic point of view of prevention of cancer metastasis. Then, we applied a high-fat diet to make mice diabetic and confirmed that a remarkable effect of metastasis suppression was available with melanoma B16-F10 (unpublished data). However, a serious problem remained that a high-fat diet increased the risk of diabetes. We, therefore, introduced a moderate hyperglycemic condition to prevent diabetes. This study aimed to examine whether melanoma metastasis could be suppressed even under such a condition.

To proceed with this study, a pre-diabetes model was essential. Pre-diabetes model mice are gene-modified mice developed by heterozygous knockout of glucokinase (*Gk*) gene (GKKO mice) and show a deficiency in glucose-stimulated insulin secretion (GSIS) [15, 16]. GKKO mice stably exhibit moderate blood glucose levels under normal diet conditions and appear to be diabetic once fed with a high-fat diet, though by adjusting the feeding period or reversing the feed type, blood glucose levels are reversible.

A melanoma cell line B16-F10 was applied to GKKO and control (Wild) mice to analyze the occurrence of metastasis in the liver, a predominant target organ. The metastatic potential of melanoma cells was quantitatively analyzed according to the method described in previous studies [17, 18]. A possible role of macrophages in suppressing metastasis was investigated by analyzing the expression of macrophage markers such as *F4/80*, *CD68* (pan-macrophage marker), *CD86* (tumor-suppressive M1-type macrophage marker), and *CD206* (tumor-promotive M2-type macrophage marker). The expression of *TNF α* and *Cxcl10* was analyzed as well to find out any involvement of cytokines and chemokines.

Materials and Methods

Animals

GKKO mice were previously developed by systemic heterozygous knockout of glucokinase (*Gk*) and regis-

tered as B6; 129-*Gck*^{mlTms} [15]. Normal littermates of GKKO mice were used as the control wild-type mice (Wild mice). All mice were bred in a specific pathogen-free room under conditions of 12 h illumination and 12 h darkness each day. Mice were fed a solid diet (MF, Oriental Yeast Co., Ltd., Tokyo, Japan) for 6–8 weeks from birth and used for cancer metastasis experiments. All animal experimental procedures were conducted according to the guidelines of the “Guide for the Care and Use of the Laboratory Animals” of Tokyo University of Agriculture and Technology, Japan, and approved by the Institutional Animal Care and Use Committee of Tokyo University of Agriculture and Technology (IACUC No. 30-40, No. 30-128, and No. R03-54).

Cell culture

Wild-type mouse melanoma cell line, B16-F10 cells were cultured in R10 medium (RPMI-1640 containing 10% fetal bovine serum (Thermo Fisher Scientific, Waltham, MA, USA) and 1% penicillin-streptomycin (Thermo Fisher Scientific)) maintained at 37°C under 5% CO₂.

Metastasis experiment

In this study, the target organ of metastasis was made only liver because of the following reasons. The liver had the highest number of metastatic colonies. The expected effect would be modest because the experimental condition was moderate hyperglycemia and not hyperglycemia. Whether the effect was suppressive or promotive depends largely on the immune response activities of target organs. Therefore, it was better to focus on a specific organ to detect a modest effect clearly. Furthermore, it was presumed that glucose metabolism was greatly involved and therefore organs with active glucose metabolism would be better.

Wild mice and GKKO mice were monitored for 4 w (Day -28~Day 0) and each mouse was challenged with PBS (250 μ l) containing 2.5×10^5 cells of B16-F10 through the tail vein at Day 0, and bred successively for 2 w (Fig. 1Aa). On Day 14, mice were euthanized, and livers were resected for metastatic analysis. Liver was cut into smaller lobes and photographed under a microscope. The number of metastatic colonies was counted, and the volume of each colony was determined. A metastatic colony was approximated as a spheroid and its volume was estimated according to the following formula [17, 18]: $V = \pi ab^2/6$, where a and b were the longest and shortest diameters, respectively measured using ImageJ software. Colonies greater than 0.0004 mm³ were counted as metastatic colonies.

Glucose tolerance test

Following an overnight fast, mice were orally administered with 2 g/kg body weight of glucose solution. Blood samples were drawn from the tail vein at 0, 15, 30, 60, 90, 120, and 180 min, respectively. Glucose concentration was measured with a G-sensor (ARKRAY Inc., Kyoto, Japan). Tests were carried out at the start of the metastasis experiment (Day -28), after 4 weeks of CD feeding and just before melanoma introduction (Day 0), and at the end of the experiment (Day 14), respectively.

RNA isolation and quantitative RT-PCR

Livers for qRT-PCR analysis were resected from mice at Day 0 to investigate the effect of moderate hyperglycemia (Fig. 1Ab). Total RNA was isolated from liver tissue using ISOGEN II (Nippongene, Tokyo, Japan) according to the manufacturer's instructions. The gene expression of *TNFA*, *Cxcl10*, *F4/80*, *CD86*, and *CD206* was quantified and normalized to that of *GAPDH* using StepOnePlus™ Real-Time PCR System (Applied Biosystems, Waltham, MA, USA). Primer sequences used are listed in Supplementary Table 1.

Western analysis

Protein samples were extracted from liver resected from mice at Day 0 (Fig. 1Ab). Livers were washed with PBS and snap-frozen with liquid nitrogen immediately upon resection. Frozen samples were grinded and homogenized using RIPA buffer (25 mM Tris-HCl, 150 mM NaCl, 1% NP-40, 1% sodium deoxycholate, 0.1% SDS, pH 7.6; Thermo Fisher Scientific). Samples were placed on ice for 30 min and sonicated (UR-20P; TOMY SEIKO, Tokyo, Japan) for a few minutes. Samples were then centrifuged at 10,000×g at 4°C for 20 min and supernatants were collected as protein samples of liver tissues. The protein concentration was determined using a TaKaRa BCA Protein Assay kit (Takara Bio Inc., Kusatsu, Japan) according to manufacturer's instructions.

A 100 µg protein solution was mixed with a 1/5 volume of 0.375 M Tris-HCl (pH 6.8) buffer solution containing 93 µg/ml DTT, 0.12 g/ml SDS, 0.6 ml/ml glycerol, and 0.6 ml/ml bromophenol blue. Then the solution was heated at 95°C for 5 min and applied to SDS-PAGE at 150 V. Protein was blotted onto a PVDF membrane at 100 V for 3 h at 4°C. The PVDF membrane was then blocked in TBS-T (Tris-buffered saline (25 mM Tris, pH 7.4, 150 mM NaCl) containing 1 (v/v)% Tween 20) solution containing 5 (w/v)% skim milk at 25°C for 30 min. Then the PVDF membrane was probed with primary antibodies against mouse B7-2 (CD86) (1:500, sc-28347; Santa Cruz Biotechnology, Dallas, TX, USA), and

GAPDH (1:1,000, sc-32233; Santa Cruz Biotechnology) in a 5% skim milk TBS-T solution at 25°C for 3 h. The membrane was further incubated with secondary antibody (anti-mouse immunoglobulin conjugated to alkaline phosphatase, Promega, Madison, WI, USA) in TBS-T at 25°C for 1 h. Finally, membranes were incubated with Western Blue Stabilized Substrate (Promega) for alkaline phosphatase at 25°C for 10 min. Targeted protein bands were quantified in relative to GAPDH bands using ImageJ software (<https://imagej.nih.gov/ij>).

Measurement of cell proliferation

B16-F10 cells were cultured in dishes (6 cm^ϕ) with R10 medium, initially containing 11 mM glucose concentration. Further, 2 M glucose solution was added to prepare R10 media containing glucose concentrations of 33 mM and 55 mM, respectively. The initial cell density was 1.0×10^5 cells/dish and cultured at 37°C under 5% CO₂. Medium change was carried out at 48 h, and the culture was continued for another 48 h. Cells were collected at 48 h and 96 h by trypsin/EDTA treatment, and cells were counted.

Wound healing assay

Migration activity was investigated by wound healing assay. B16-F10 cells were cultured in R10 media containing glucose concentrations of 11 mM, 33 mM, and 55 mM, respectively, on a 12-well plate at 37°C under 5% CO₂. The initial cell density was 2.0×10^5 cells/well. Cells were cultured for 48 h to obtain 100% confluency. A uniform scratch was made down the center of each well using a sterile micropipette tip, and scraped cells were removed by washing with a phosphate-buffered solution (PBS). After adding R10 medium, the culture was continued for 24 h. The wound area of each well was measured at 0, 4, 6, 12, and 24 h, respectively, using ImageJ software.

Transwell invasion assay

Transwell invasion assay was performed using 6.5 mm transwell inserts (Corning®, Glendale, AZ, USA) with 8.0 µm pore polycarbonate membrane. Inserts were treated beforehand with Matrigel™ Matrix Basement Membrane (BD Biosciences, Franklin Lakes, NJ, USA) in coating buffer (250 µg/ml) and incubated for 2 h. B16-F10 cells were cultured in serum-free media for 48 h and were collected by trypsin/EDTA treatment. Cells collected were suspended in serum-free media containing glucose concentrations of 11 mM, 33 mM, and 55 mM. 5.0×10^4 cells were seeded in the upper chamber of the insert and complete R10 media were added in the lower chamber. After 22 h of incubation, the leftover cells in

the upper chamber were discarded using a cotton bud, and cells on the lower surface were fixed with 100% methanol and stained with hematoxylin and eosin solutions. Ten random fields of each membrane were observed and photographed under a microscope with 4× magnification. Cells were then analyzed and counted.

Statistical analysis

All data were given as mean ± SD or mean ± SEM as stated in each result figure. Outliers were determined by a Smirnov-Grubbs test to be greater than 0.05 one-tailed probability. The statistical significance between two specific data groups was analyzed by paired two-tailed Student's *t* test. Results of *in vivo* metastasis experiments were expressed by boxplots and the statistical significance between medians was analyzed by Wilcoxon test using R (ver.4.1.1). The statistical significance level was denoted by a *p*-value or the following marks: ***: $P < 0.001$, **: $P < 0.01$, *: $P < 0.05$, †: $P < 0.1$, #: $P < 0.2$. Also, in the case of $P > 0.2$, numerical values of *P* were shown up to about 0.3.

Results

In vivo test results of the effects of moderate hyperglycemia on the metastasis of B16-F10 cells to liver

The effects of hyperglycemia on the metastasis of melanoma were estimated by three *in vivo* tests for body weight, glucose tolerance, and metastatic colony formation. At first, the body weight change was measured to estimate the effect on the basic growth process. There was no abnormality in the weight gain process (Fig. 1B). The body weight gain speed of GKKO mice became slightly higher than that of Wild mice, which was observed after Day -7. This seemed to reflect a higher activity of glucose metabolism in GKKO mice than in Wild mice. At Day 0, melanoma cells were introduced in mice but its effect on the weight gain speed was not observed.

Next, the glucose tolerance test was conducted to confirm that hyperglycemic condition could be maintained stably in GKKO mice. The glucose tolerance was quantified from the area under the curve (AUC) of the glucose concentration profile (Fig. 1C). The AUC values of GKKO mice were greater than those of Wild mice (Fig. 1D). AUC values of both mice groups were stable throughout the test of metastasis from Day -28 to Day 14.

Finally, the analysis of metastatic colonies was conducted with resected livers (Fig. 1E). The number of metastatic colonies in Wild mice group ranged from 128

to 697 and its median was 419 (Fig. 1F). In contrast in GKKO mice group, the median of the number of colonies was 240. Similarly, the volume of metastatic colonies in GKKO mice group also decreased (Fig. 1G). The effect of moderate hyperglycemia on the number of metastatic colonies estimated from the relative values of the median was 0.61-fold suppression in statistical significance at $P = 0.06$. Such a suppression effect of moderate hyperglycemia on the metastasis of melanoma was a new finding.

Involvement of *TNFα*, *Cxcl10*, and macrophage markers

Under hyperglycemic conditions, active glucose metabolism is accompanied by an inflammatory response, which is presumed to affect metastasis. It is believed that the organ most affected by such effects is the liver. Therefore, inflammation-dependent factors were analyzed with resected liver. The expression of *TNFα* and *Cxcl10* in GKKO mice seemed to be slightly higher than that in Wild mice, but no statistical significance was obtained (Figs. 2A and B). This indicates that no severe inflammation was formed in the liver under a moderate hyperglycemic condition. On the other hand, an outstanding result was obtained with macrophage markers. Pan-macrophage markers such as *F4/80* and *CD68* showed an increasing tendency under a moderate hyperglycemic condition (Figs. 2C and D), suggesting immune cell activation. Moreover, the expression of *CD86* (a tumor-suppressive M1-type macrophage marker) was upregulated (Fig. 2E) but contrarily the expression of *CD206* (a tumor-promotive M2-type macrophage marker) was downregulated under a moderate hyperglycemic condition (Fig. 2F). These strongly suggest a functional role of macrophages in suppressing the metastasis of melanoma. The highest significance ($P < 0.01$) was observed in the expression of the upregulation of *CD86*. Then the expression of *CD86* protein was analyzed by western analysis and its increase under a moderate hyperglycemic condition was confirmed (Fig. 2G). This finding suggests that anti-tumor immunization was activated in GKKO mice.

In vitro test results of the effects of glucose conditions on the metastasis-associated properties of B16-F10 cells

Metastatic potential of B16-F10 cells was profoundly suppressed in GKKO mice liver and the suppression seems highly related to the increase in anti-tumor phenotype macrophages. However, the direct impact of the moderate hyperglycemic condition on melanoma itself has yet to be known. Therefore, the proliferation, migra-

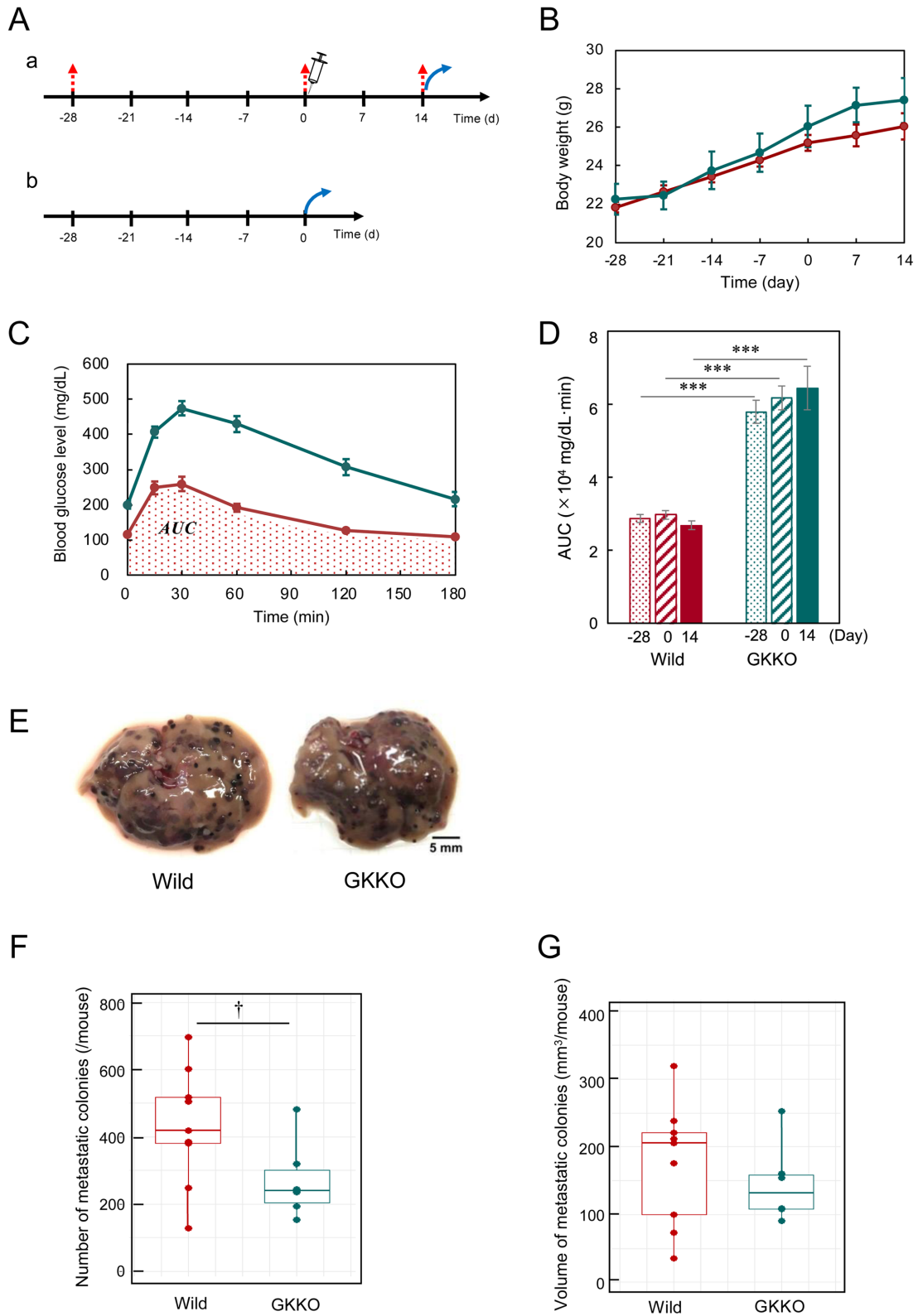


Fig. 1. Metastatic potential of B16-F10 cells in Wild and GKKO mice. (A) Schedule of glucose tolerance tests (a) and liver resection for qRT-PCR (b). (Red arrow), the tail intravenous injection of B16-F10 cells (syringe), and the resection of liver (blue arrow). (B) Body weight of mice. Body weight of mice were measured once per week throughout the metastasis experiment. (C) Glucose concentration changes during glucose tolerance test conducted at Day 0. Red line: Wild, green line: GKKO. Dotted area indicates the area under the curve (AUC) for Wild mice. (D) AUC values obtained in (C) at Day-28, 0, and 14, respectively. Bars & lines: mean \pm SEM for $n=9$ (Wild), 6 (GKKO). (E) Images of the liver with metastatic colonies of B16-F10. Scale bar: 5 mm. (F) The number of metastatic colonies per mouse. (G) The total volume of metastatic colonies per mouse. Number of mice tested: $n=9$ (Wild), 6 (GKKO).

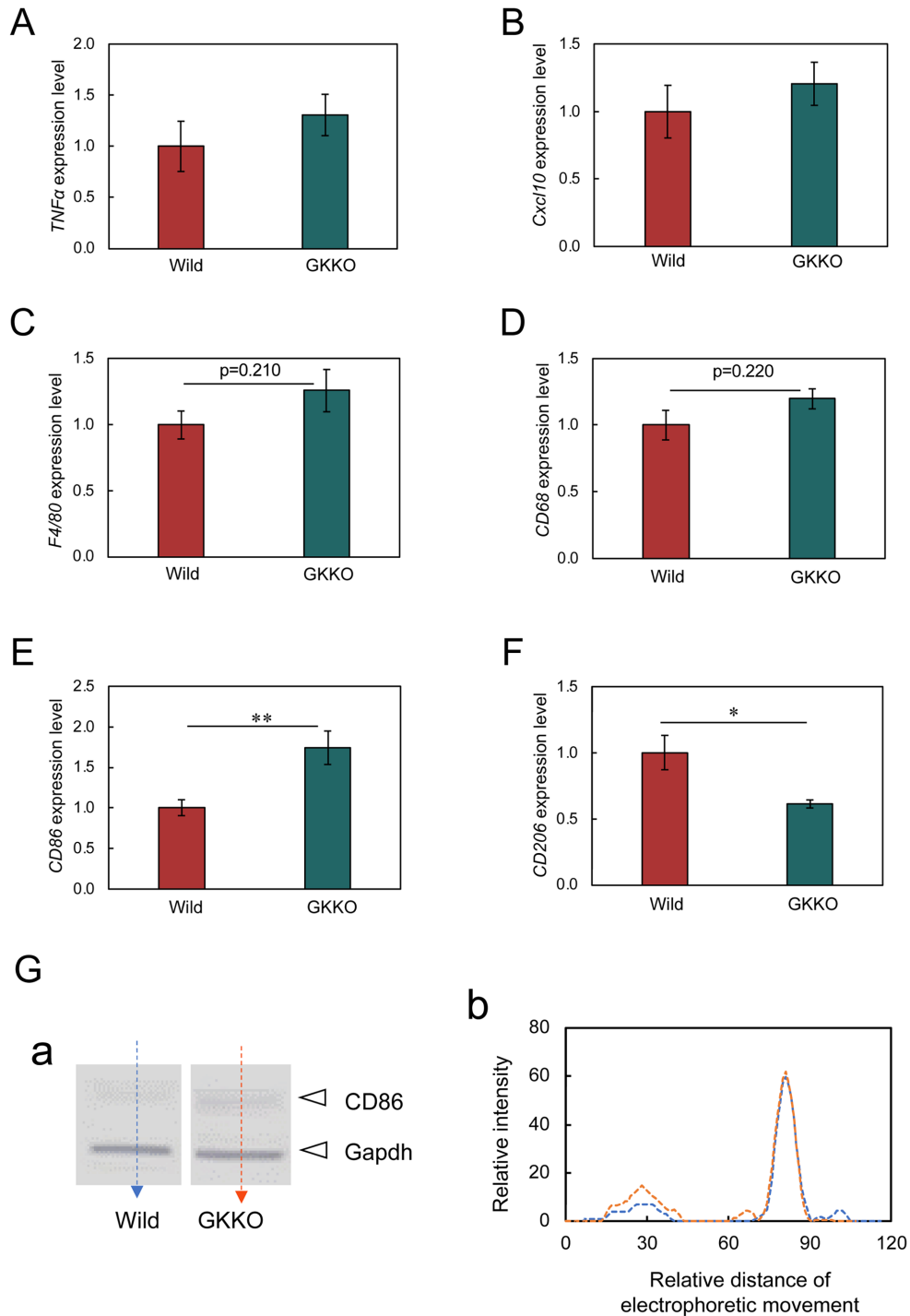


Fig. 2. Effects of moderate hyperglycemia on the expression of *TNF α* , *Cxcl10*, and macrophage markers in the liver. (A) *TNF α* expression. (B) *Cxcl10* expression. (C–F) macrophage markers. Every gene expression intensity was normalized to that of *GAPDH*. Bars are mean \pm SEM, $n=3$ (*TNF α*), $n=6$ (*Cxcl10*, *F4/80*, *CD68*, *CD86*, *CD206*). (G) Protein band of CD86 and GAPDH of Wild and GKKO mice liver samples (a) and their intensity profiles analyzed using ImageJ (b). Blue dotted line: Wild, red dotted line: GKKO.

tion, and invasion activities of B16-F10 cells were investigated at glucose concentrations of 11 mM (a normal condition), 33 mM (a moderate hyperglycemic condition), and 55 mM (a hyperglycemic condition), respectively.

A high value of proliferation means that cancer cells grow rapidly at the metastasized spot. At 11 mM, the number of cells was initially 1.0×10^5 cells/dish and increased to 29.8×10^5 cells/dish at 96 h (Fig. 3A). At higher concentrations, the number of cells became

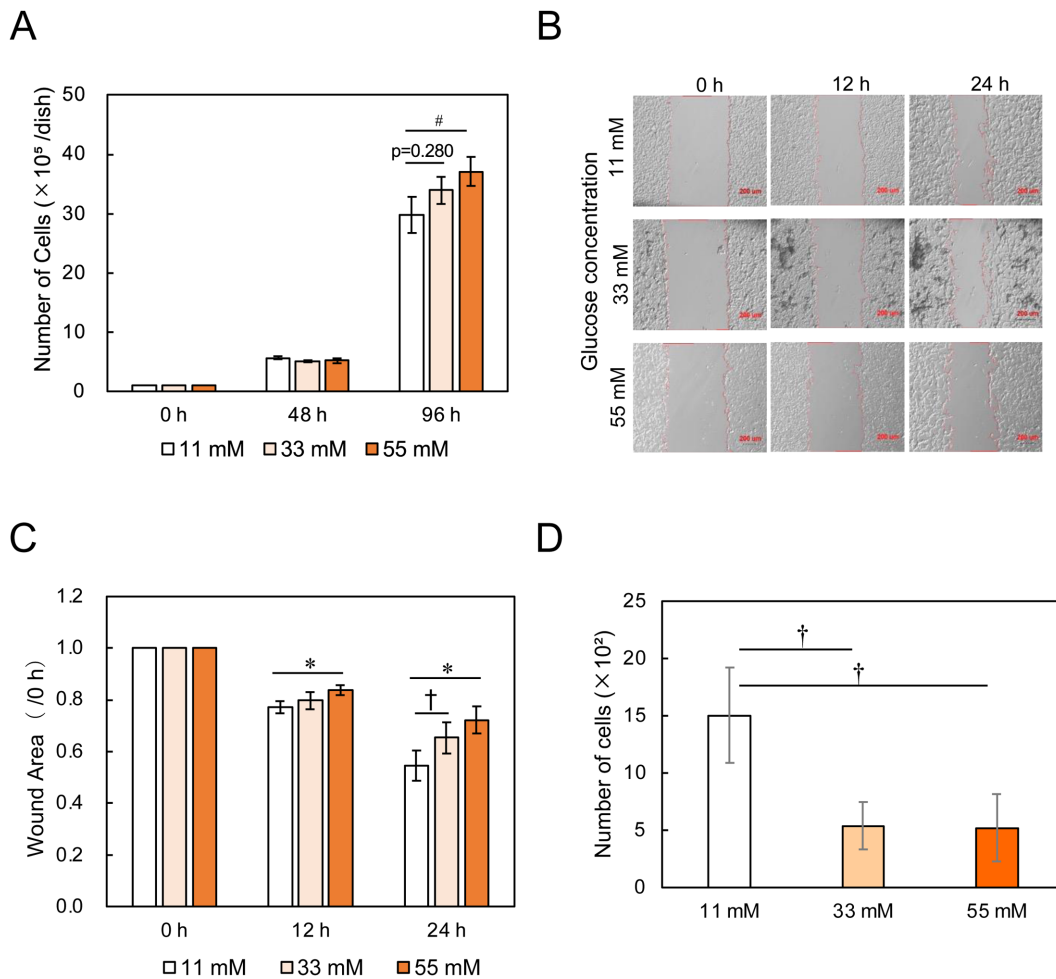


Fig. 3. Effects of glucose concentrations on the metastasis-associated *in vitro* properties of B16-F10 cells. (A) Cell proliferation. Bars are mean \pm SD, for $n=3$. (B) Microscopic images of wound areas in the migration assay. Scale bar: 200 μ m. (C) Cell migration activity. Bars are mean \pm SD, for $n=4$. (D) Cell invasion activity. Bars are mean \pm SD, for $n=3$.

greater. Therefore, cell proliferation was promoted by high glucose.

High migration activity means that cancer cells are active in free space and was investigated by wound healing assay. The width of the wound was initially about 800 μ m. During culture, the cells migrated from both edges of the wound, and the wound width became narrower accordingly (Fig. 3B). The ratio of the wound area at each time point to the initial wound area was defined as migration activity, indicating that the smaller the ratio, the higher the migration activity. The migration rate at 11 mM was 45%/24 h (wound area=0.55), while it decreased to 35%/24 h (wound area=0.65) and 28%/24h (wound area=0.72) at 33 mM and 55 mM, respectively (Fig. 3C). Therefore, the cell migration was suppressed by high glucose.

High invasion activity means that the movement of cancer cells to push through intercellular space is active and was investigated by Transwell invasion assay. B16-

F10 cells were cultured in a serum-free medium containing 11 mM, 33 mM, or 55 mM glucose in the upper chamber of Transwell insert. The initial number of cells cultured was 5.0×10^4 cells/insert. The number of cells which passed through the Matrigel-coated membrane at 11 mM was 1.5×10^3 . In contrast, the cell number decreased to 0.5×10^3 cells at higher glucose concentrations (Fig. 3D). Therefore, the invasion activity of B16-F10 cells was markedly suppressed by high glucose.

In summary, the results of migration and invasion activities pre-estimated the metastasis suppression by moderate hyperglycemia. These properties of B16-F10 clearly contrasted those of other cancers.

Discussion

In the studies that have been conducted so far to investigate the relationship between diabetes and cancer metastasis, there seems to have been no idea that diabe-

tes must be suppressed. However, in the prognostic life of cancer treatment, even for the prevention of metastasis, the risk of diabetes should not be increased at the same time. In this study, we succeeded in discovering conditions that can meet this demand for the first time by using pre-diabetic model mice.

The effect of suppressing metastasis was obtained primarily due to the properties of the cancer cells themselves. All the previous studies on cancer metastasis under hyperglycemia were conducted under conditions of high blood glucose levels of diabetes. Among them, metastasis inhibitory effect was observed only in one case each of melanoma [13] and colon cancer [14]. In other words, these two types of cancer cells are considered to have the property of being more sensitive to hyperglycemia and more strongly affected by it than other cancer cells. In fact, metastasis-related cellular activities of melanoma showed a slight increase in proliferative ability, but a marked decrease in migratory and invasive abilities. It should be stressed that a sufficiently large reduction ($P<0.01$) in invasion ability was observed even at moderate hyperglycemia levels.

A larger factor underpinning the anti-metastasis effect is the immune response, in which macrophages play a large role [19]. In response to the metastasized cancer cells, macrophages favor a pro-inflammatory phenotype and express M1 markers to disrupt cancer cells. Under hyperglycemic conditions, glucose is actively metabolized in normal tissue cells, regardless of whether cancer cells are present. As a result, active oxygen is generated and causes inflammation. This leads to the suppression of metastasis when cancer cells are present. At the same time, the counter effects of anti-inflammatory conditions are also worth considering. Glucocorticoids, for instance, are anti-inflammatories used in cancer treatment [20] but activate gluconeogenesis causing blood glucose increase. The analysis of substantial roles of glucocorticoids will provide useful information on this point.

In the GKKO mice, systemic heterozygous knockout of the *Gk* gene leads to poor glucose signaling in pancreatic β cells, hence impairing insulin secretion [15, 21]. As a result, the blood glucose level is maintained at a moderate hyperglycemic level throughout the whole body. Even at such a moderate level, inflammation will occur although its extent might be lower. Consequently, macrophages are likely to increase pro-inflammatory functions, accompanied by an increase in the expression of M1 type markers.

Macrophages in livers are mostly Kupffer cells and the rest is bone-marrow-origin monocytic cells. Based on liver injury models, it was revealed that both Kupffer cells and monocytic cells showed similar profiles of

surface markers such as CD86, CD163, and CD206 [22]. The expression of CD86⁺macrophage is necessary for proliferation and cytokine production. CD163⁺macrophage expression is involved in bacterial recognition and local inflammatory reactions. Also, the expression of CD206⁺macrophage is often required for phagocytosis, antigen presentation, and clearance of pro-inflammatory mediators. According to the M1-M2 criteria, CD86⁺macrophage is a M1 type and CD163⁺macrophage and CD206⁺macrophage are M2 types, although the functional properties may not strictly be distinguished between M1 and M2 [23].

In this study, we observed the enhanced expression of *CD86* ($P<0.01$) and the suppressed expression of *CD206* ($P<0.05$) in macrophages in the liver in response to moderate hyperglycemia. Moreover, the expression of pro-inflammatory *TNF α* and *Cxcl10* tended to increase although statistically not significant. These responses may be understood to be the pro-inflammatory and consequently tumor-suppressive functions of CD86⁺macrophage and CD206⁺macrophage. Such understanding is supported by the following reports.

One report concerns the suppression of liver cancer that is known to be promoted by intestinal flora-derived toxins [24]. This toxin-promoting liver cancer could be suppressed by the antibiotic ciprofloxacin via upregulating *CD86* and downregulating *CD206* [25]. Another report demonstrated the suppression of metastasis of colorectal cancer [14]. High-fat diet induced the conversion of adipose tissue macrophages from M1 type (CD206⁺macrophage) to anti-tumor M1 type (CD206⁻macrophage) through TLR4/*Cxcl10* axis. *Cxcl10* was generated by M1 macrophage-activated T cells, which prevented metastasis.

In summary, a postulated mechanism of the metastasis suppression effect under moderate hyperglycemia in GKKO mice liver is illustrated in Fig. 4.

During the prognostic period, patients are recommended to take a highly nutritious diet to improve their health. In that case, however, special care must be taken not to increase the risk of diabetes. The present study demonstrated a possibility that melanoma B16-F10 did not make moderate hyperglycemia in mice worse, supporting no risk of diabetes, and that metastasis of B16-F10 to liver was suppressed under the moderate hyperglycemic condition in mice. These should contribute to dietary planning during prognosis.

Conflict of Interest

The authors declare that they have no conflict of interest.

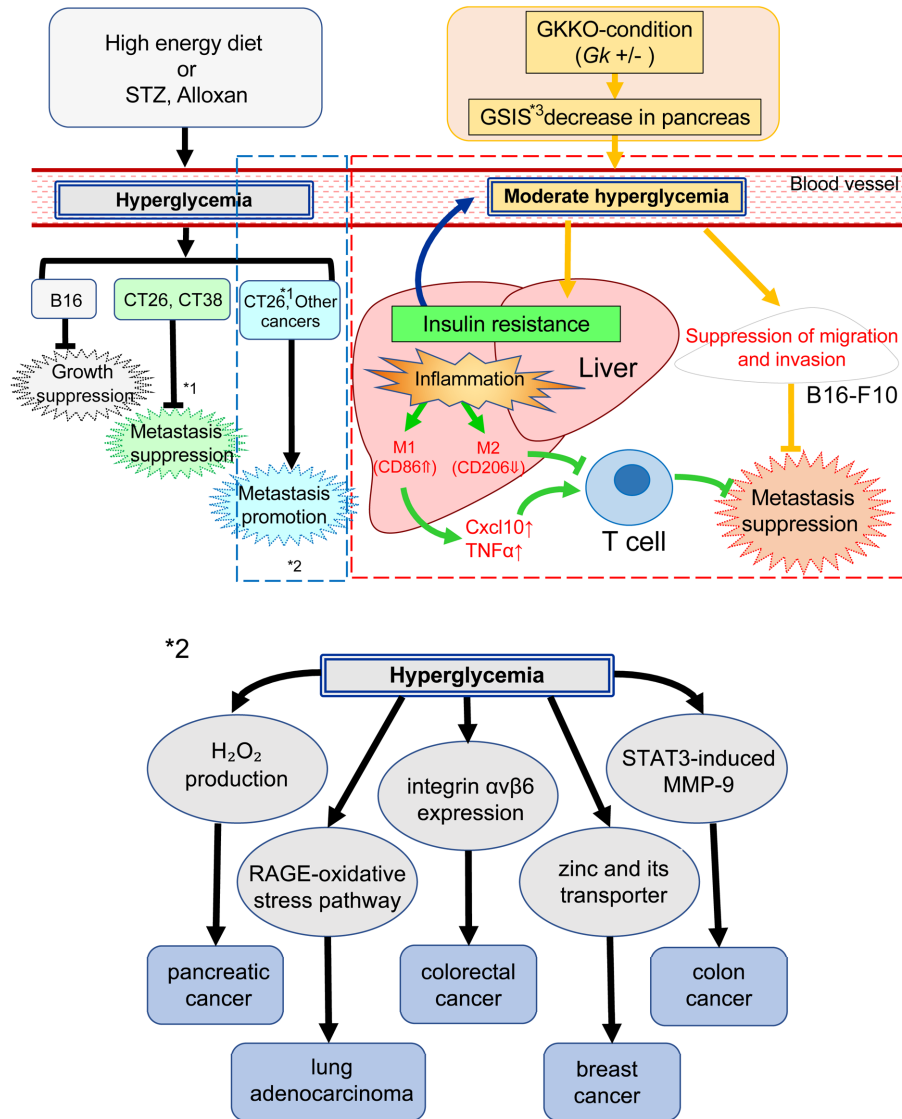


Fig. 4. A postulated scheme of suppression of melanoma B16-F10 by moderate hyperglycemia. Left side: Previous results of melanoma (B16), colorectal cancer (CT26, CT38), and other type of cancer conducted under hyperglycemic conditions. *1. Metastasis of CT26 was suppressed in high fat diet fed mice but promoted in STZ-induced hyperglycemic mice. *2. Details of inside a blue dotted box. Right side (inside a red dotted box): Present result of melanoma (B16-F10) conducted under moderate hyperglycemic conditions. *3. GSIS: glucose-stimulated insulin secretion.

Acknowledgments

We thank Prof. Emer. Hideaki Matsuoka of Tokyo University of Agriculture and Technology for his valuable advice about statistical analysis.

References

1. Gray-Schopfer V, Wellbrock C, Marais R. Melanoma biology and new targeted therapy. *Nature*. 2007; 445: 851–857. [Medline] [CrossRef]
2. Gallagher EJ, LeRoith D. Obesity and diabetes: the increased risk of cancer and cancer-related mortality. *Physiol Rev*. 2015; 95: 727–748. [Medline] [CrossRef]
3. Kasuga M, Ueki K, Tajima N, Noda M, Ohashi K, Noto H,

et al. Report of the JDS/JCA joint committee on diabetes and cancer. *Diabetol Int*. 2013; 4: 81–96. [CrossRef]

4. Luc K, Schramm-Luc A, Guzik TJ, Mikolajczyk TP. Oxidative stress and inflammatory markers in prediabetes and diabetes. *J Physiol Pharmacol*. 2019; 70: 809–824. [Medline]
5. Kang Q, Yang C. Oxidative stress and diabetic retinopathy: Molecular mechanisms, pathogenetic role and therapeutic implications. *Redox Biol*. 2020; 37: 101799. [Medline] [CrossRef]
6. Clemmer JS, Xiang L, Lu S, Mittwede PN, Hester RL. Hyperglycemia-mediated oxidative stress increases pulmonary vascular permeability. *Microcirculation*. 2016; 23: 221–229. [Medline] [CrossRef]
7. Li W, Ma Q, Li J, Guo K, Liu H, Han L, et al. Hyperglycemia enhances the invasive and migratory activity of pancreatic cancer cells via hydrogen peroxide. *Oncol Rep*. 2011; 25: 1279–1287. [Medline]

8. Li W, Zhang L, Chen X, Jiang Z, Zong L, Ma Q. Hyperglycemia promotes the epithelial-mesenchymal transition of pancreatic cancer via hydrogen peroxide. *Oxid Med Cell Longev*. 2016; 2016: 5190314. [[Medline](#)] [[CrossRef](#)]
9. Liao YF, Yin S, Chen ZQ, Li F, Zhao B. High glucose promotes tumor cell proliferation and migration in lung adenocarcinoma via the RAGE-NOXs pathway. *Mol Med Rep*. 2018; 17: 8536–8541. [[Medline](#)]
10. Wang B, Wang S, Wang W, Liu E, Guo S, Zhao C, et al. Hyperglycemia promotes liver metastasis of colorectal cancer via upregulation of integrin $\alpha\beta 6$. *Med Sci Monit*. 2021; 27: e930921. [[Medline](#)] [[CrossRef](#)]
11. Takatani-Nakase T, Matsui C, Maeda S, Kawahara S, Takahashi K. High glucose level promotes migration behavior of breast cancer cells through zinc and its transporters. *PLoS One*. 2014; 9: e90136. [[Medline](#)] [[CrossRef](#)]
12. Lin CY, Lee CH, Huang CC, Lee ST, Guo HR, Su SB. Impact of high glucose on metastasis of colon cancer cells. *World J Gastroenterol*. 2015; 21: 2047–2057. [[Medline](#)] [[CrossRef](#)]
13. Pavelić J, Benković B, Pavelić K. Growth and treatment of B16 melanoma in hyperglycemic mice. *Res Exp Med (Berl)*. 1980; 177: 71–78. [[Medline](#)] [[CrossRef](#)]
14. Xiang W, Shi R, Zhang D, Kang X, Zhang L, Yuan J, et al. Dietary fats suppress the peritoneal seeding of colorectal cancer cells through the TLR4/Cxcl10 axis in adipose tissue macrophages. *Signal Transduct Target Ther*. 2020; 5: 239 [[CrossRef](#)]. [[Medline](#)]
15. Saito M, Kaneda A, Sugiyama T, Iida R, Otokuni K, Kaburagi M, et al. Production of a mouse strain with impaired glucose tolerance by systemic heterozygous knockout of the glucokinase gene and its feasibility as a prediabetes model. *Exp Anim*. 2015; 64: 231–239. [[Medline](#)] [[CrossRef](#)]
16. Lu B, Kurmi K, Munoz-Gomez M, Jacobus Ambuludi EJ, Tonne JM, Rakshit K, et al. Impaired β -cell glucokinase as an underlying mechanism in diet-induced diabetes. *Dis Model Mech*. 2018; 11: dmm033316. [[Medline](#)] [[CrossRef](#)]
17. Saito M, Kishi R, Sasai T, Hatakenaka T, Matsuki N, Minagawa S. Effect of Nanog overexpression on the metastatic potential of a mouse melanoma cell line B16-BL6. *Mol Cell Biochem*. 2021; 476: 2651–2661. [[Medline](#)] [[CrossRef](#)]
18. Hatakenaka T, Matsuki N, Minagawa S, Khoo CSM, Saito M. Anti-metastatic function of extracellular vesicles derived from *Nanog*-overexpressing melanoma. *Curr Oncol*. 2022; 29: 1029–1046. [[Medline](#)] [[CrossRef](#)]
19. Rasheed A, Rayner KJ. Macrophage responses to environmental stimuli during homeostasis and disease. *Endocr Rev*. 2021; 42: 407–435. [[Medline](#)] [[CrossRef](#)]
20. Timmermans S, Souffriau J, Libert C. A general introduction to glucocorticoid biology. *Front Immunol*. 2019; 10: 1545. [[Medline](#)] [[CrossRef](#)]
21. Gorman T, Hope DC, Brownlie R, Yu A, Gill D, Löfvenmark J, et al. Effect of high-fat diet on glucose homeostasis and gene expression in glucokinase knockout mice. *Diabetes Obes Metab*. 2008; 10: 885–897. [[Medline](#)] [[CrossRef](#)]
22. Elchaninov AV, Fatkhudinov TK, Vishnyakova PA, Lokhovina AV, Sukhikh GT. Phenotypical and functional polymorphism of liver resident macrophages. *Cells*. 2019; 8: 1032. [[Medline](#)] [[CrossRef](#)]
23. Murray PJ, Allen JE, Biswas SK, Fisher EA, Gilroy DW, Goerdts S, et al. Macrophage activation and polarization: nomenclature and experimental guidelines. *Immunity*. 2014; 41: 14–20. [[Medline](#)] [[CrossRef](#)]
24. Yu LX, Schwabe RF. The gut microbiome and liver cancer: mechanisms and clinical translation. *Nat Rev Gastroenterol Hepatol*. 2017; 14: 527–539. [[Medline](#)] [[CrossRef](#)]
25. Fan M, Chen S, Weng Y, Li X, Jiang Y, Wang X, et al. Ciprofloxacin promotes polarization of CD86⁺CD206⁺ macrophages to suppress liver cancer. *Oncol Rep*. 2020; 44: 91–102. [[Medline](#)] [[CrossRef](#)]